Parasitology Research (2019) 118:289–306
https://doi.org/10.1007/s00436-018-6163-5

IMMUNOLOGY AND HOST-PARASITE INTERACTIONS - ORIGINAL PAPER

# Characterization of metalloproteases and serine proteases of *Toxoplasma gondii* tachyzoites and their effect on epithelial cells

Carlos J. Ramírez-Flores[1] · Rosalba Cruz-Mirón[1] · Rossana Arroyo[2] · Mónica E. Mondragón-Castelán[1] · Tais Nopal-Guerrero[1] · Sirenia González-Pozos[3] · Emmanuel Ríos-Castro[4] · Ricardo Mondragón-Flores[1]

Received: 4 June 2018 / Accepted: 22 November 2018 / Published online: 1 December 2018


## Abstract

*Toxoplasma gondii* can infect all nucleated cells from warm-blooded organisms. After infection, *Toxoplasma* spreads throughout the body and migrates across biological barriers, such as the intestinal and blood-brain barriers, as well as the placenta in pregnant women. The mechanisms for parasite dissemination are still unknown; however, proteases could play a role as a virulence factor. The aim of this study was to detect and to characterize proteases in whole-cell extracts and in excretion/secretion products from tachyzoites of the RH strain isolated from infected mice. Both fractions were analyzed by gelatin and casein zymography and by azocasein degradation. The biochemical characterization of proteases included standardization of optimal conditions for their activation, such as pH, the presence of cofactors, and a reducing agent. In both fractions, we detected at least nine gelatin-degrading metalloproteases in the range of 50 to 290 kDa. The proteases present in the excretion/secretion products were found as soluble proteins and not associated with exosome-like vesicles or other secretory vesicles. Moreover, by using casein zymography, it was possible to detect three serine proteases. Exposure of MDCK cells to excretion/secretion products modified the organization of the cell monolayer, and this effect was reverted after washing thoroughly with PBS and inhibition by metalloprotease and serine protease inhibitors. Proteomic analysis of excretion/secretion products identified 19 proteases. These findings suggest that tachyzoites of a highly virulent strain of *Toxoplasma* use a battery of proteases to modify the epithelium, probably as a strategy to facilitate their tissue dissemination.

**Keywords** Epithelial alteration · Exosome-like vesicles · Excretion/secretion products · Proteases · *Toxoplasma gondii* Zymography

## Introduction

*Toxoplasma gondii* can infect and replicate within any nucleated cells from warm-blooded organisms (Tenter et al. 2000). After infection, parasites invade and proliferate within enterocytes, and then, they disseminate to all organs, reaching even distant and immune-privileged organs such as the brain and eyes shortly after infection (Barragán and Sibley 2002, 2003; Harker et al. 2015). During tissue dissemination, *Toxoplasma* uses a paracellular pathway that involves ICAM-1 on the membrane of the host cell and the parasite adhesin MIC2 to transmigrate across polarized monolayers (Barragán et al. 2005). Interestingly, parasites are able to transmigrate without modifying the epithelium integrity (Barragán et al. 2005), although in the retinal pigment epithelium, the parasites induce changes in the tight junction complex with an increase in paracellular permeability (Nogueira et al. 2016).

Section Editor: Daniel K Howe

**Electronic supplementary material** The online version of this article (https://doi.org/10.1007/s00436-018-6163-5) contains supplementary material, which is available to authorized users.

✉ Ricardo Mondragón-Flores
rmflores@cinvestav.mx

[1] Departamento de Bioquímica, Centro de Investigación y de Estudios Avanzados del Instituto Politécnico Nacional (CINVESTAV-IPN), Av. IPN No. 2508, Col. Zacatenco, C.P. 07360 Ciudad de México, Mexico

[2] Departamento de Infectómica y Patogénesis Molecular, CINVESTAV-IPN, Ciudad de México, Mexico

[3] Unidad de Microscopía Electrónica, LaNSE, CINVESTAV-IPN, Ciudad de México, Mexico

[4] Unidad de Genómica, Proteómica y Metabolómica, LaNSE, CINVESTAV-IPN, Ciudad de México, Mexico

Extracellular and intracellular parasites use different molecular mechanisms for spreading through tissues, including proteolytic degradation of extracellular matrix (ECM) by cysteine proteases (CPs), serine proteases (SPs), and metalloproteases (MPs) that have been found to be related to their virulence (Cuellar et al. 2017; Hernández-Gutiérrez et al. 2004; Khan and Siddiqui 2009; McGwire et al. 2003). Furthermore, infection by the intracellular parasites, *Plasmodium falciparum* (Prato et al. 2005) and *T. gondii* (Buache et al. 2007; Schuindt et al. 2012), has been proposed to stimulate the biosynthesis of MPs by the host cell in order to degrade ECM proteins, facilitating the transmigration of infected leukocytes. Threonine (TPs) and glutamic proteases have been poorly studied in protozoans.

In *Toxoplasma*, proteases have been reported to be important not only for invasion but also for protein processing. We know the invasion depends on SPs because specific inhibitors block it (Conseil et al. 1999). In addition, knocking out subtilisin-like SP (TgSUB1) altered the processing of MIC2, MIC4, and M2AP, resulting in reduced adhesion to and invasion of the host cells (Lagal et al. 2010). TgSUB2 is known to be involved in the proteolytic maturation of rhoptry proteins (Miller et al. 2003).

The rhomboid family of *T. gondii* includes an SP that has been shown to be involved in the processing of MIC proteins (Buguliskis et al. 2010). CPs have been demonstrated to be involved in invasion and digestion of host proteins (Dou et al. 2014; Que et al. 2007). In addition, five genes encoding cathepsins (TgCPs) have been reported, i.e., three cathepsins C (TgCPC1, C2, and C3), one cathepsin B (TgCPB), and one cathepsin L (TgCPL). TgCPB and TgCPL colocalize within an acidic vacuolar compartment (VAC) (Dou et al. 2013). Their inhibition by vinyl sulfone affects the invasion, and they have been considered as potential vaccine antigens against toxoplasmosis (Chaparro et al. 2018; Han et al. 2017; Zhao et al. 2013).

MPs also contribute to parasite virulence. Toxolysin 4 (TLN4) from micronemes is secreted by tachyzoites in the presence of high $Ca^{2+}$ and during the invasion; however, its function remains unknown (Laliberte and Carruthers 2011), while TLN1 has been shown to be involved in the processing of rhoptry proteins (Hajagos et al. 2012). In addition, aspartic proteases (APs) have been associated with the dense granule export machinery of *Toxoplasma* (Coffey et al. 2015) and with immune protection (Zhao et al. 2017). Immunization of mice with the aspartic protease 3 of *Toxoplasma* increased their survival after infection up to 18 days (Zhao et al. 2017). Nevertheless, these proteases have not been found to play a role in the dissemination process or evasion of the immune response.

Zymography is a powerful method widely used for the detection of proteases and characterization of different properties such as optimal pH, cofactors, and sensitivity to specific inhibitors in different cell types, as well as in extracellular (de Sousa et al. 2010; Louie et al. 2002; Monte et al. 2017) and intracellular parasites (Nogueira de Melo et al. 2010). In previous reports, three proteases sensitive to $Ca^{2+}$ and to MP inhibitors were detected by zymography in excretion/secretion products (E/S products) but not in whole-cell extracts (WE) of *T. gondii* tachyzoites of the RH strain (Ahn et al. 2001; Song and Nam 2003). A recent report, based on in silico analysis, showed the identification of 49 genes encoding different MPs that are transcribed in tachyzoites (RH strain), although their function and biochemical properties remain to be determined (Escotte-Binet et al. 2018).

In the present study, we characterized the activity of proteases from a highly pathogenic strain (RH) of *Toxoplasma* in WE and E/S products of tachyzoites isolated from infected mice. The biochemical characterization of the proteases was done by (a) zymography using different substrates and (b) azocasein degradation assays. The identification of the protease families was conducted with specific inhibitors. The identities of the proteases present in the E/S products were determined by mass spectrometry (MS). In addition, the effect of the proteases on the integrity and spatial organization of the actin cytoskeleton of MDCK epithelial cells was evaluated.

## Materials and methods

### Animals

BALB/c mice were maintained under regulated environmental conditions (temperature, humidity, and filtered air) in an animal facility. Handling was performed according to the Mexican Official Norm (NOM-062-ZOO-1999) for the production, care, and use of laboratory animals.

### Parasites and host cells

Tachyzoites of the RH strain of *T. gondii* were propagated in female BALB/c mice by peritoneal infection as previously reported (Mondragón and Frixione 1996). Parasites harvested from peritoneal exudates were thoroughly washed with PBS (138 mM NaCl, 1.1 mM $K_2HPO_4$, 0.1 mM $Na_2HPO_4$, and 2.7 mM KCl, pH 7.2) by low-speed centrifugation and then by filtration through 5-μm pore polycarbonate filters (Millipore Co., MA). Parasites were used within 4 h after isolation.

The MDCK cells (ATCC-CCL 34) were grown in Dulbecco's Minimum Essential Medium (DMEM, Sigma-Aldrich, Co., St. Louis, MO), supplemented with 10% fetal bovine serum (FBS) and 2 mM L-glutamine (GIBCO, BRL), under a 5% $CO_2$ atmosphere at 37 °C. The viability of the tachyzoites and the MDCK cells was determined by exclusion of trypan blue dye and SYTOX green dead cell stain (Eugene, OR) according to the manufacturer. Parasites and MDCK cells were used with not less than 96% viability.

## Preparation of whole-cell extracts

For zymography, $1 \times 10^7$ tachyzoites were solubilized in zymography buffer (125 mM Tris-HCl at pH 6.8, 4% SDS, 20% glycerol, and 0.002% bromophenol blue) without reducing agents and without boiling. For Western blot (WB), tachyzoites were solubilized in lysis buffer (2% β-mercaptoethanol, 1% SDS, 20 mM EGTA, 2 mM Tris-HCl at pH 7.5, 0.1 mM PMSF, 0.1 mM TPCK, and 0.1 mM TLCK), sonicated in ice for 15 s at 40 Hz (in a ultrasonic processor, model GE 130PB Cole-Parmer, Vernon Hills, USA), and then centrifuged at 16,500×*g* at 4 °C. The supernatant was used as WE and the protein concentration was determined by the Bradford method.

## Preparation of excretion/secretion products

Tachyzoites ($2 \times 10^7$) were maintained in 100 μl of sterile MEM with no serum for 4 h at 37 °C and then centrifuged at 510×*g*. The E/S products (supernatants) were recovered and filtered through 0.22-μm pore polycarbonate filters. Presence of remnant parasites was corroborated by observation in a phase contrast microscope. E/S products were precipitated at 4 °C with a mixture of methanol/chloroform, centrifuged, and the pellet was resuspended in zymography buffer or in lysis buffer for WB. As negative control, tachyzoites were fixed with 1% glutaraldehyde in PBS for 1 h at room temperature (RT), then washed and blocked with PBS and 0.5% BSA, respectively. The fixed parasites were subjected to the protocol followed to obtain E/S products.

## One-dimension gel electrophoresis

Proteins obtained from WE or E/S products were electrophoretically separated by 7.5% SDS-PAGE. Gels were stained with Coomassie blue R-250 dye (Neuhoff et al. 1988), silver dye, or transferred to nitrocellulose (NC) membranes for WB.

## One-dimension gelatin zymography

Zymographies were performed as previously reported (Heussen and Dowdle 1980) with modifications. Briefly, 0.1% gelatin (type A: porcine skin, Sigma-Aldrich, Co.) or 0.1% casein (Sigma-Aldrich, Co.) was copolymerized in 7.5% SDS-PAGE gel. Electrophoresis was carried out under nonreducing conditions, and the gels were washed out in renaturation buffer (100 mM Tris-HCl at pH 7.5 and 2.5% Triton X-100) to remove SDS. To determine the optimal activation pHs, gels were incubated at 37 °C in the following activation buffers: (a) 10 mM sodium acetate at pH 3.5 (Oliveira-Jr et al. 2013), (b) 10 mM Tris-HCl at pH 5.5 (Oliveira-Jr et al. 2013), (c) 100 mM Tris-HCl at pH 7.5 (Saboia-Vahia et al. 2013), and (d) 50 mM Tris-HCl at pH 8.0 (Sampieri et al. 2010) in the absence or in presence of $MgCl_2$ (1, 5, and 10 mM), $CaCl_2$ (1, 5, and 10 mM), $ZnCl_2$ (0.5 and 5 μM), and DTT (1 and 5 mM). Gels were stained with Coomassie blue dye, and proteolytic degradations were seen as clear bands contrasting with the blue background of the gel. The respective electrophoretic patterns were obtained by SDS-PAGE without substrates. Urea 4 M was added to the zymography buffer in order to discard the existence of protease oligomers. Trypsin, MS grade (Sigma-Aldrich, Co.), was used as positive control with a degradation band of approximately 25 kDa.

Gels were digitalized in a gel-imaging system (EZ Imager, BioRad, Hercules, CA) and the molecular weights of the proteolytic bands were obtained by using the Image Lab Software Version 4.1 from the GelDoc system with a pre-stained protein ladder (New England Biolabs, MA). The molecular weights of the proteolytic bands in substrate gels do not necessarily correspond to the molecular weights of a regular SDS-PAGE.

To identify the protease families, specific inhibitors were added to the renaturation and the activation buffers. Inhibitors included the following: for MPs, EGTA (1 and 5 mM) and 1,10-phenanthroline (1 and 5 mM); for SPs, TLCK (1 and 5 mM), TPCK (1 and 5 mM), and PMSF (1 and 5 mM); for CPs, E-64 (1 and 5 μM); and for APs, pepstatin A (1 and 5 μM). Vehicles were used as controls at the highest concentrations.

## Azocasein assay

Azocasein degradation by spectrophotometry was used to detect proteases not evidenced by zymography (Coelho et al. 2016; Gimenez et al. 2000; Tork et al. 2016). Proteolytic activity was analyzed in WE from $2 \times 10^7$ tachyzoites as well as in E/S products harvested from $5 \times 10^7$ tachyzoites. Azocasein assays were carried out at 37 °C for 24 h in TBS (20 mM Tris-HCl at pH 7.5, 1 mM $CaCl_2$, 1 μM $ZnCl_2$) and 1% azocasein (Sigma-Aldrich, Co.). The reaction was stopped by addition of 25% TCA at 4 °C; the sample was vortexed and centrifuged at 16,100×*g* for 5 min. Absorbance was measured in the supernatant at 335 nm and normalized to a blank reaction. Identification of proteases was done by adding specific inhibitors to the reaction volume. The enzymatic activities without protease inhibitors were considered as 100% of the activity (maximal activity). The substrate degradation obtained in presence of the inhibitors with respect to the maximal activity was expressed as the residual activity. Statistical analysis was carried out using GraphPad Prism version 6 (GraphPad Software, San Diego, CA).

## Western blot analysis

Twenty micrograms of WE or E/S products was separated by SDS-PAGE and then transferred to NC membranes. Strips

were blocked by incubation with 6% skim milk dissolved in TBS-T (10 mM Tris-HCl, 75 mM NaCl, and 0.1% Tween 20 at pH 8.0) and then incubated with the corresponding primary antibodies. Once thoroughly washed, the strips were incubated with secondary antibodies conjugated to the horseradish peroxidase (HRP). The reaction was detected by chemiluminescence using the ECL Western blotting analysis system kit (GE, Buckinghamshire, UK). Rabbit polyclonal antibody anti-GAPDH was purchased from Santa Cruz Biotechnology (USA) and anti-Lamin B1 and anti-H3 histone were purchased from Abcam (UK). Mouse monoclonal antibody anti-β-tubulin were purchased from Invitrogen (Frederick, MD). Rabbit polyclonal antibody anti-ARO and mouse monoclonal antibody anti-MIC2 were generously donated by D. Soldati (Dept. MIMOL, UNIGE, CH). Antibodies anti-MIC1 and anti-MIC3 were generously donated by C. Mercier (Chem, Biol Dept., U. Grenoble, FRA).

## Effect of E/S products on the integrity of epithelial cells

Approximately, $1 \times 10^9$ tachyzoites were harvested from infected mice and maintained for 4 h at 37 °C in sterile DMEM without serum ($1 \times 10^8$ tachyzoites/ml) and E/S products were obtained as above. E/S products (20 μg/ml) were added to MDCK monolayers and then incubated for 1, 2, and 4 h, replacing the E/S products every 1 h. When required, E/S products were incubated with protease inhibitors, 10 mM PMSF, 10 mM 1,10-phenanthroline, or 5 μM E-64 for 1 h at 4 °C, precipitated with a mixture of methanol/chloroform, resuspended in DMEM without serum, and then added to the MDCK cells. Precipitation of the E/S products by methanol/chloroform mixture did not modify the proteolytic activities and it was a strategy necessary to avoid adverse effects of the cell monolayer by the inhibitors. As controls, cell monolayers were treated for 4 h with (a) E/S products from tachyzoites prefixed, (b) E/S products inactivated by heat (96 °C for 1 h), or (c) DMEM without serum. After treatment, MDCK monolayers were processed for scanning electron microscopy (SEM) as below indicated.

## Effect of E/S products in the distribution of F-actin in MDCK cells

After treatment of MDCK with E/S products, cells were fixed with 4% PFA, permeabilized with 0.04% NP40, and then blocked with 1% BSA at RT. Cells were stained with rhodamine phalloidin, washed with PBS, and then counterstained with DAPI. Cells were imaged by confocal microscopy (LSM700 Zeiss, Carl Zeiss, DEU). The thickness of the epithelium was measured in the 3D projections using the Zen imaging software (Carl Zeiss) in at least ten different zones. The mean thickness and the statistical analysis was carried out using GraphPad Prism version 6.

## Subcellular fractionation of E/S products

Approximately $1 \times 10^9$ tachyzoites were harvested from infected mice and maintained for 4 h at 37 °C in sterile PBS ($3 \times 10^8$ tachyzoites/ml) then sequentially centrifuged at 200×*g* at 4 °C for 10 min, 10,000×*g* at 4 °C for 10 min, and 150,000×*g* at 4 °C for 70 min twice as reported (Li et al. 2017). The pellet with exosome-like vesicles and the supernatant with soluble components were recovered and processed for gelatin zymography and for transmission electron microscopy (TEM) as below indicated.

## Electron microscopy

1. To observe the effect of the E/S products on the MDCK cells (see above), cells were thoroughly washed with PBS, fixed with 2.5% glutaraldehyde, post-fixed with 1% $OsO_4$, washed with PBS, and then dehydrated under increasing concentrations of ethanol. Samples were critical-point dried with $CO_2$ in a Samdry-780 A equipment (Tousimis Research, Rockville, MD), gold-sputtered in a Denton Vacuum Desk II (Denton Vacuum, Moorestown, NJ), and viewed in an SEM JSM-6510-LV (JEOL LTD, Japan).
2. To visualize exosome-like vesicles, aliquots of supernatant or pellet obtained after fractionation (see above) were deposited on formvar-covered nickel grids and then negatively stained with 1% aqueous uranyl acetate for TEM imaging in a JEM 1400 (JEOL LTD).
3. To observe parasites during the secretion process, extracellular tachyzoites were maintained in PBS for different times at 37 °C and then processed for TEM or SEM. Tachyzoites were fixed with 2.5% glutaraldehyde, post-fixed with 1% $OsO_4$, and then dehydrated in increasing concentrations of ethanol. Parasites were gradually embedded in increasing concentrations of Spurr's resin (EMS, Hatfield, PA) and then polymerized for 48 h at 60 °C. Thin sections were obtained in a Reichert Jung ultramicrotome (Wien) and then stained with saturated uranyl acetate and lead citrate. Parasites were then analyzed and imaged by TEM. For SEM, parasites previously fixed and dehydrated were critical-point dried with $CO_2$ and gold-sputtered and then imaged in the SEM. As a negative control, freshly harvested tachyzoites were washed, immediately fixed, and processed for SEM.

## Identification of proteases in E/S products by MS analysis

Thirty micrograms of E/S products was loaded on a 10% SDS-PAGE and then left to advance for about 1 cm within the gel. The band containing all the proteins was cut and enzymatically digested according to a modified protocol

(Shevchenko et al. 2006). Concentrated tryptic peptides were loaded into a symmetry C18 trap V/M precolumn (Waters, Milford, MA): 180 μm × 20 mm, 100 Å pore size, 5 μm particle size desalted using as a mobile phase A, 0.1% formic acid (FA) in $H_2O$ and mobile phase B, and 0.1% FA in acetonitrile (ACN) under the isocratic gradients 99.9% mobile phase A and 0.1% of mobile phase B at a flow of 5 μl/min during 3 min. Then, peptides were loaded and separated in an HSS T3 C18 column (Waters): 75 μm × 150 mm, 100 Å pore size, 1.8 μm particle size, using an UPLC ACQUITY M-Class (Waters) with the same mobile phases under the following gradient: 0 min 7% B, 121.49 min 40% B, 123.15 to 126.46 min 85% B, and 129 to 130 min 7% B, at a flow of 400 nL/min and 45 °C. The spectral data were acquired in a mass spectrometer with electrospray ionization (ESI) and ion mobility separation (IMS) Synapt G2-Si (Waters) using data-independent acquisition (DIA) approach by $HDMS^E$ mode (Waters). The tune page for the ionization source was set with the following parameters: 2.60 kV in the sampling capillary, 30 V in the sampling cone, 30 V in the source offset, 70 °C for the source temperature, 0.6 bar for the nanoflow gas, and 120 L/h for the purge gas flow. Two chromatograms were acquired (low- and high-energy chromatograms) in positive mode in a range of *m/z* 50–2000 with a velocity of 0.5 scans/s. No collision energy was applied to obtain the low-energy chromatogram, while for the high-energy chromatograms, the precursor ions were fragmented using a collision energy ramp of 19–55 V. Generated raw files containing MS and MS/MS spectra were deconvoluted and compared using ProteinLynx Global Server (PLGS) v3.0.3 software (Li et al. 2009) (Waters) against a reversed *T. gondii* GT1 database (downloaded from ToxoDB, Release 38, 19 June 2018). Workflow parameters included trypsin as a cutting enzyme and prediction of one missed cleavage site in tryptic peptides, carbamidomethyl (C) as a fixed modification and amidation (N-term), and deamidation (N, Q), oxidation (M), and phosphoryl (S, T, Y) as variable modifications: automatic peptide and fragment tolerance and minimum fragment ion matches per peptide, 2; minimum fragment ion matches per protein, 5; minimum peptide matches per protein, 1; and a false discovery rate (FDR) ≤ 4%. All identifications had a percentage of ≥ 95% of reliability (Protein AutoCurate green). Synapt G2-Si was calibrated with [$Glu^1$]-Fibrinopeptide, $[M+2H]^{2+}$ = 785.84261 at ≤ 1.5 ppm.

The prediction of the subcellular localization of the proteases identified by MS was done by using the DeepLoc-1.0 web server (available in http://www.cbs.dtu.dk/services/DeepLoc) (Almagro Armenteros et al. 2017) and using the Protist Secretome and Subcellular Proteome KnowledgeBase (ProtSecKB) for *T. gondii* (available in http://proteomics.ysu.edu/secretomes/protist/index.php). The ID and the amino acid sequence (FASTA format) for every protein were obtain from ToxoDB data base (available in toxodb.org, Release 39, 30 August 2018).

## Results

### Proteolytic profile by gelatin zymography in WE from tachyzoites

The presence of proteases in WE from tachyzoites (RH strain) isolated from infected mice was tested by gelatin zymography at different pH values (3.5, 5.5, 7.5, and 8.0) in the absence of reducing agents or cofactors. Activating conditions for proteases at pH 3.5 or pH 5.5 did not show degradation bands in the zymography gel (Fig. 1a). At pH 7.5 and 8.0, at least three slight degradation bands of approximately 84 kDa and two close bands of approximately 290 kDa were detected (Fig. 1a, arrows). Trypsin (Tryp), used as a control, produced a consistent degradation band of approximately 25 kDa at neutral pH (Fig. 1a**,** arrow, 25 kDa). Trypsin was assayed in all of the following experiments as a positive control, but its results are not shown in the respective figures.

### Effect of cofactors and incubation time on the proteolytic activity of WE from tachyzoites

To determine the contribution of cofactors and to optimize the gelatinolytic activity, the following cofactors were tested in WE from tachyzoites: $CaCl_2$ (0, 1, 5, and 10 mM), $MgCl_2$ (1, 5, and 10 mM), and $ZnCl_2$ (0.5, 1, and 5 μM) at pH 5.5, 7.5, and 8.0 (Fig. 1b–d). The presence of $CaCl_2$ at the different concentrations and pH values tested produced seven clear degradation bands of approximately 290, 254, 199, 172, 110, 84, and 75 kDa, with maximal proteolytic activities at pH 7.5 and pH 8.0 (Fig. 1c, d). The presence of $MgCl_2$ did not show degradation bands under any of the conditions evaluated. The addition of 1 μM $ZnCl_2$ produced two faint proteolytic bands of approximately 84 and 290 kDa only at pH 7.5 (Fig. 1c, $ZnCl_2$, arrows). The addition of DTT to identify CPs (Wilkesman 2017) did not show proteolytic degradations (Fig. 1b, DTT). Based on these results, the optimal conditions chosen for zymography were 1 mM $CaCl_2$ and 1 μM $ZnCl_2$ at pH 7.5. To determine the optimal activation time for detection of proteases, we tested for 1, 3, 6, 8, 12, 18, and 24 h under the optimal incubation conditions (Fig. 2a). The clearest gelatin degradation occurred at 24 h with a proteolytic profile of at least nine proteases of approximately 290, 254, 199, 172, 110, 84, 75, 59, and 50 kDa. Proteases of high molecular weight were not considered to be oligomers since the proteolytic profile was not affected by the addition of 4 M urea to the zymography buffer (Online Resource 1**,** inset a).

To eliminate the possibility that the proteolytic pattern corresponds to peritoneal proteases from the mice, peritoneal exudates were harvested from noninfected mice previously injected with mineral oil via i.p. to induce inflammation. The gelatin zymogram showed two proteases in the range of 42–45 kDa (Fig. 2b**,** PP; arrows) that were not in the proteolytic profile observed in WE from tachyzoites (Fig. 2b**,** TP). In addition, the mixture of

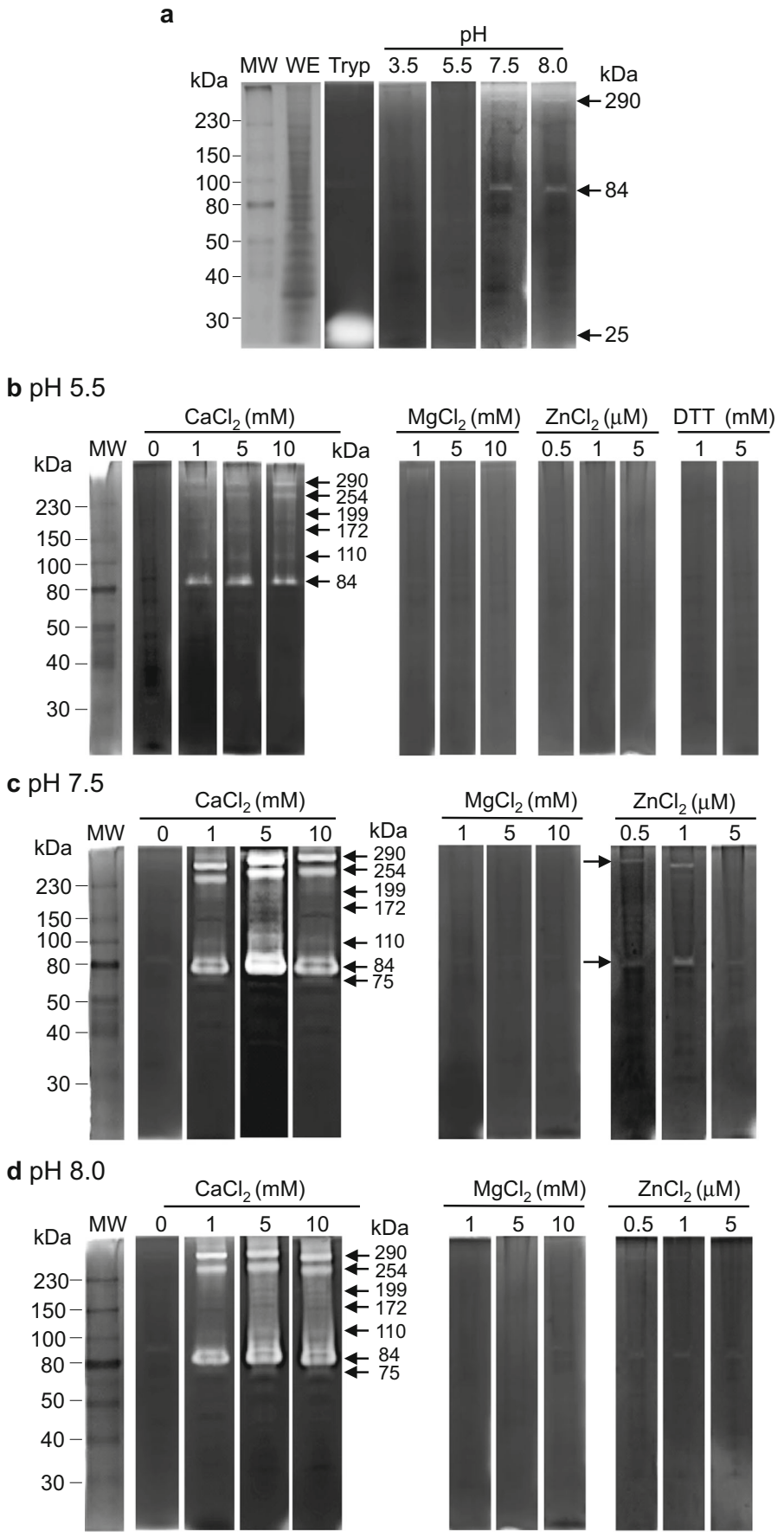
a
pH
MW WE Tryp 3.5 5.5 7.5 8.0
kDa
kDa
230
150
100
80
50
40
30
290
84
25
b pH 5.5
CaCl2 (mM)
MgCl2 (mM)
ZnCl2 (μM)
DTT (mM)
MW 0 1 5 10
1 5 10
0.5 1 5
1 5
kDa
290
254
199
172
110
84
c pH 7.5
75
d pH 8.0

◀ **Fig. 1** Gelatin zymogram of WE of tachyzoites at different pH, cofactors, and a reducing agent. Zymograms of WE of $1 \times 10^7$ tachyzoites were evaluated at pH 3.5, 5.5, 7.5, and 8.0 (**a**–**d**, respectively) at different concentrations of $MgCl_2$, $ZnCl_2$, $CaCl_2$, or DTT. WE indicates the electrophoretic pattern. Trypsin in **a** (Tryp) was used as a positive control. MW, molecular weight

equivalent amounts of proteins from peritoneal exudate from the noninfected mouse and WE from tachyzoites showed the additive pattern of proteases from both sources (Fig. 2b, PP/TP). These results indicate that the parasite purification discarded the proteases from the host peritoneal exudate and that the proteases described in the WE were exclusively from the parasite.

## Metalloproteases were detected in WE from tachyzoites by gelatin zymography

The identification of the protease family in WE from tachyzoites was done with specific inhibitors for the four families of proteases: AP, CP, MP, and SP as reported in other cell models (Madanan and Mechoor 2017; Saboia-Vahia et al. 2014; Song and Nam 2003). The presence of inhibitors for MPs, EGTA, and 1,10-phenanthroline produced a complete inhibition of all of the nine protease bands even at the lowest inhibitor concentrations, indicating that the proteases belong to the MP family (Fig. 2c, MP). In contrast, inhibitors of AP (pepstatin A), SP (PMSF, TPCK, and TLCK), and CP (E-64) did not affect the proteolytic degradation of gelatin at the various concentrations evaluated (Fig. 2c). The different solvents (water, methanol, and isopropanol) used to dissolve the respective inhibitors had no effect on the proteolytic pattern (Online Resource 1, inset b).

## Metalloproteases of *T. gondii* are also released as E/S products

Proteases were searched for in the E/S products at different times (from 5 min to 4 h) by SDS-PAGE and gelatin

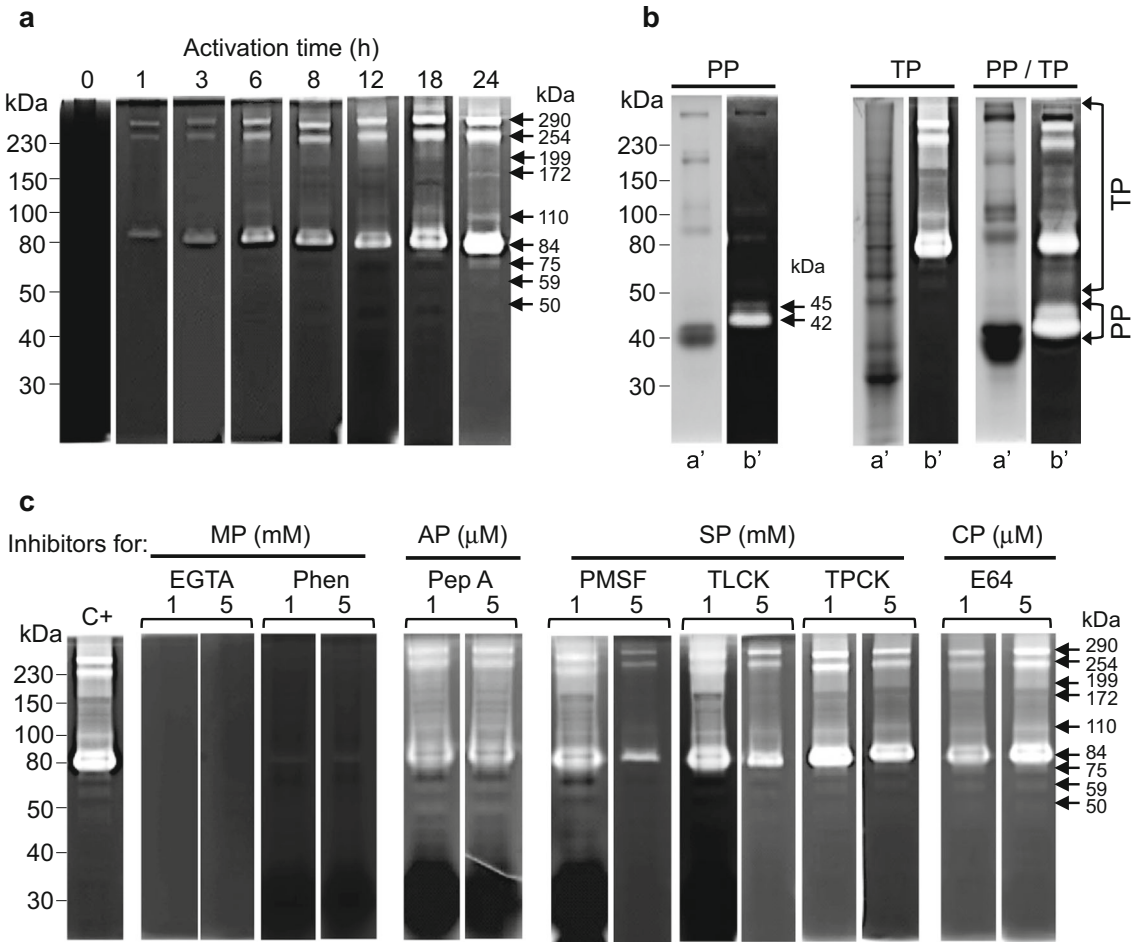


**Fig. 2** Activation time of proteases from WE, determination of their source, and identification of the protease families with specific inhibitors. **a** Zymogram of WE evaluated at different activation times from 0 to 24 h at 37 °C under optimal conditions for activation. **b** PAGE-SDS (a′) and gelatin zymograms (b′) of (PP) peritoneal proteins from healthy mice injected with mineral oil; (TP) WE of tachyzoites and (PP/TP) proteins from the peritoneal fluid mixed with proteins of the WE. **c** Effect of inhibitors of the four families of proteases: MP, metalloproteases; AP, aspartic proteases; SP, serine proteases; and CP, cysteine proteases on the proteolytic activity of WE. C+, corresponds to WE without protease inhibitors

zymography under the optimal activation conditions previously determined (Fig. 3). The electrophoretic profile of the E/S proteins as well as the proteolytic profile seen in the zymogram progressively increased in intensity as secretion time increased (Fig. 3a). No later harvesting times were considered to conserve the viability of the parasites. The proteolytic pattern from E/S products showed the same pattern of proteolytic bands found in WE, of approximately 290, 254, 199, 172, 110, 84, and 75 kDa; however, the proteolytic bands of 54 and 50 kDa were present in a very low intensity (Fig. 3a, double head arrows). When the amount of E/S products tested was increased, the same number of bands were observed in WE and E/S products (Online Resource 2, insets a and b).

Proteases detected in the E/S products were not released by parasitic lysis, as demonstrated by the absence of cytosolic proteins (GAPDH and β-tubulin) from *T. gondii* as well as the absence of proteins associated with cytosolic organelles such as TgARO from the cytoplasmic face of the rhoptries, lamin B1 (a nuclear cytoskeleton protein), and histone H3, all of these checked for by WB in E/S products harvested at 4 h (Fig. 3b). In contrast, the secretory proteins TgMIC1, TgMIC2, and TgMIC3 were clearly found in the E/S products (Fig. 3b). Furthermore, no parasites were detected to be undergoing necrotic processes, and no cytosolic vacuolization was observed by phase contrast microscopy. As expected, a negative control of parasites fixed with glutaraldehyde did not show E/S products at any of the evaluated times (data not shown). E/S products from parasites suspended in MEM and immediately harvested did not show proteolytic activity (considered to be time 0). The viability of the tachyzoites determined by the exclusion of trypan blue and SYTOX green dye was between 96 and 99% even after 4 h under secretion conditions (Online Resource 3).

Incubation of the E/S products with inhibitors for MPs (EGTA and 1,10-phenanthroline) inhibited all of the proteolytic degradation bands (Fig. 3c), indicating that these proteases corresponded to MPs. No effects were observed with the other inhibitors tested (Fig. 3c; AP, SP, and CP).

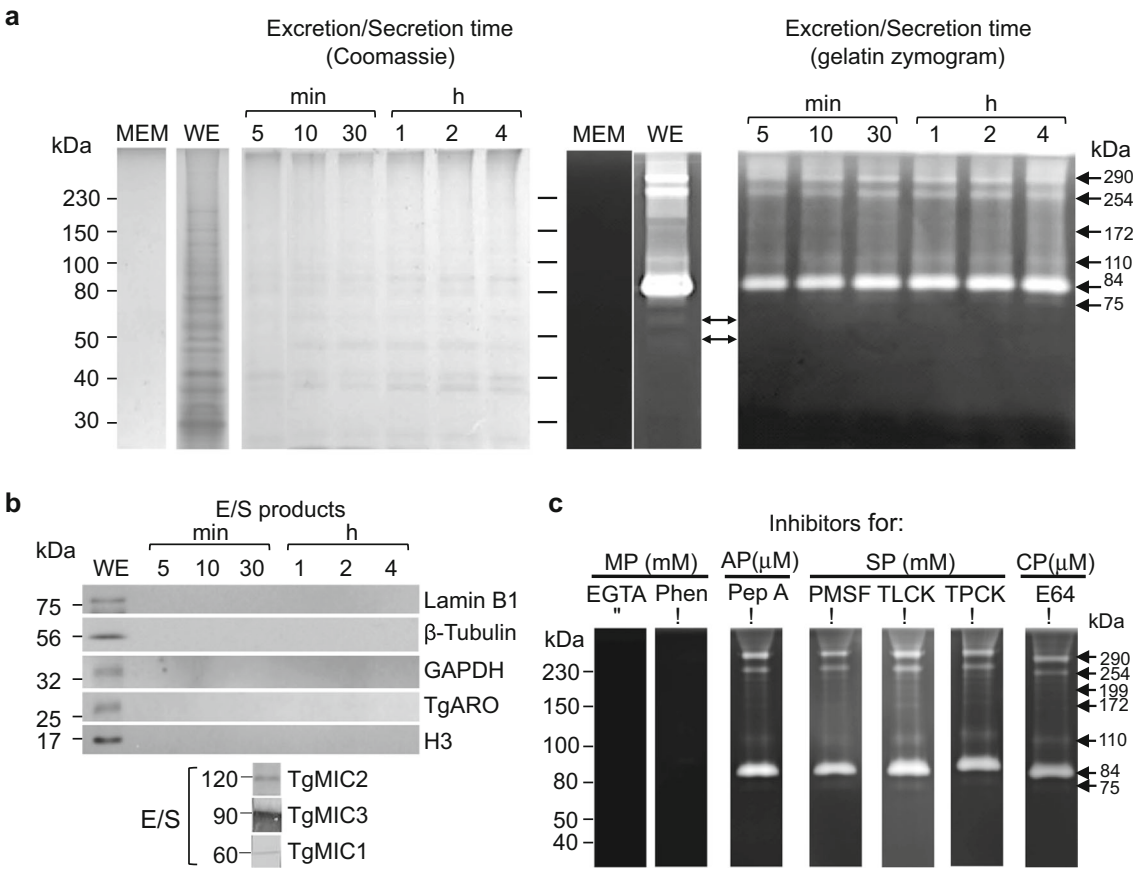


**Fig. 3** Proteases released in E/S products are not the result of cell lysis and they were sensitive to metalloprotease inhibitors. **a** Silver staining of SDS-PAGE and the respective gelatin zymogram of E/S products harvested at different times. Double-headed arrows indicate proteases detected in WE and E/S products. MEM corresponds to time 0 of excretion/secretion. **b** Detection by WB of Lamin B1, β-tubulin, GAPDH, TgARO, and H3 proteins as control of no lysis in WE and E/S products harvested at different times; TgMIC1, TgMIC2, and TgMIC3 were detected as a control of secreted proteins. **c** Effect of protease inhibitors for MP, AP, SP, and CP on the proteolytic profile of E/S products

## Metalloproteases and serine proteases were detected by degradation of azocasein

To extend the search for proteases in *T. gondii* tachyzoites, we tested WE and E/S products for the degradation of azocasein as detected by spectrophotometry. A clear degradation of azocasein was detected in both sources (labeled as PBS), and it was defined as 100% of the activity (Fig. 4a, b). The evaluation of azocasein degradation in the presence of the MP inhibitors, EGTA and 1,10-phenanthroline, in WE showed a reduction by approximately 60 and 90% of the substrate degradation, respectively (Fig. 4a), while with the E/S products, the inhibition was approximately 75 and 90%, respectively (Fig. 4b). The addition of the SP inhibitor, PMSF, to WE showed a clear reduction of azocasein degradation of approximately 70%, while TPCK had no effect, and with TLCK, only partial inhibition was observed. In E/S products, PMSF inhibited approximately 70% of the proteolytic degradation of the substrate, while TLCK and TPCK diminished the substrate degradation by approximately 30 and 50%, respectively. The CP inhibitor E-64 did not affect the azocasein degradation in WE or in E/S products (Fig. 4a, b). When a mixture of inhibitors at optimal concentrations (1,10

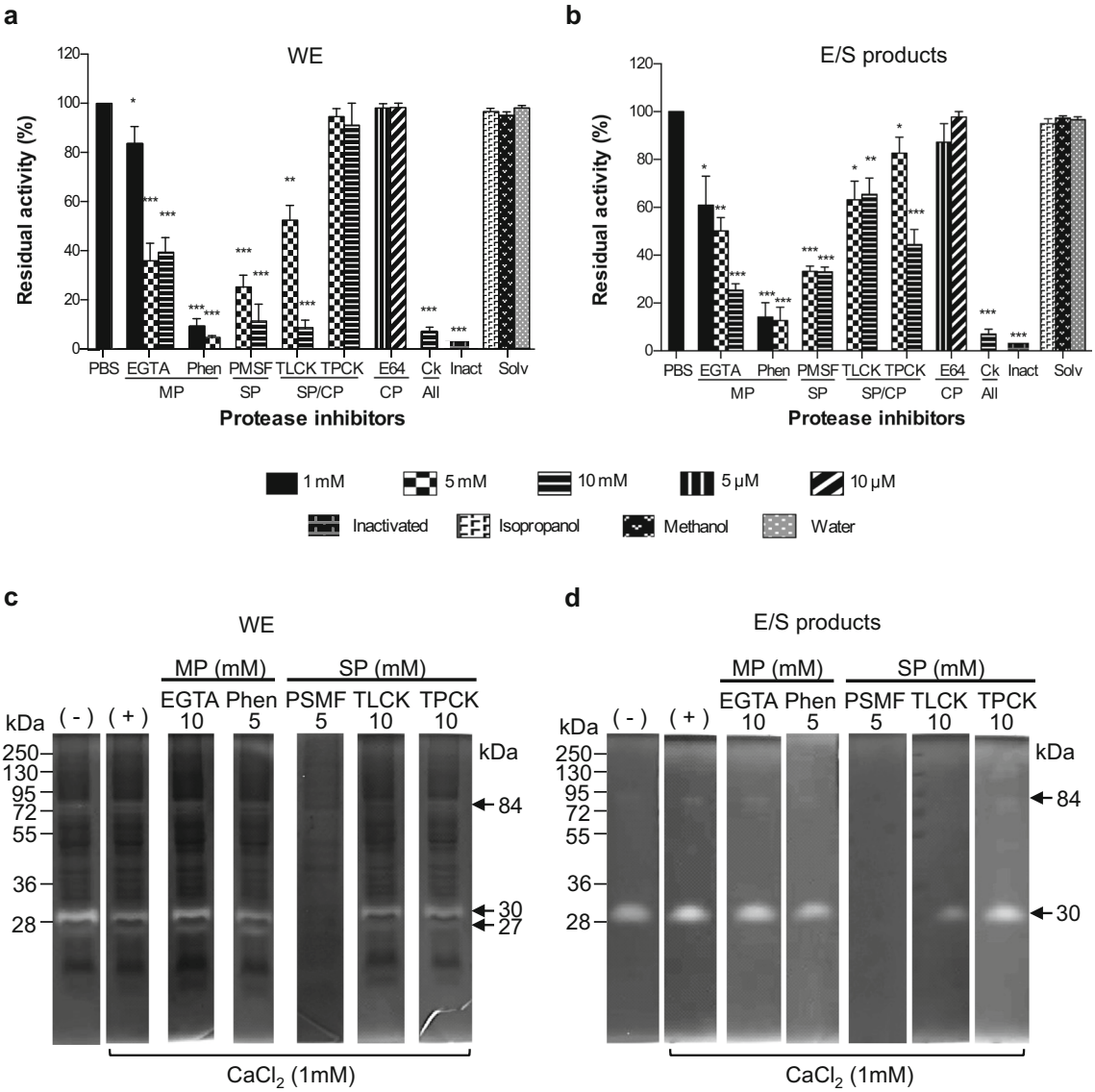


**Fig. 4** Degradation of azocasein and casein by WE and E/S products. Effect of protease inhibitors in azocasein degradation in **a** WE from $2 \times 10^7$ tachyzoites and **b** E/S products from $5 \times 10^7$ tachyzoites. PBS in WE and E/S products corresponds to control condition in absence of protease inhibitors. Inact corresponds to WE and E/S products analyzed after inactivation by heat. Solv corresponds to the solvents of the respective inhibitors; Ck, cocktail of protease inhibitors used in the assay. Bars indicate standard deviation; Statistic analysis was performed by using the *T* test with $*p < 0.05$, $**p < 0.005$, and $***p < 0.0005$. **c** and **d** correspond to the casein zymograms of WE of $1 \times 10^7$ tachyzoites and E/S products of $2 \times 10^7$ tachyzoites respectively with protease inhibitors. Lanes (+) and (−) correspond to zymograms controls done in absence or in presence of $Ca^{2+}$ without protease inhibitors

phenanthroline, EGTA, TPCK, TLCK, and E-64) was incubated with WE and E/S products, only approximately 10% of the substrate was degraded in both cases, indicating that the whole degradation capability was determined by the presence of all of the proteases (Fig. 4a, b, All). These results indicate that MP and SP are active in WE and in E/S products. A negative control with samples previously heated did not show proteolytic activity (Fig. 4a, b, Inact). The solvents used to dissolve the inhibitors did not affect the degradation of the substrate (Fig. 4a, b, Solv).

## Serine proteases are detected by casein zymography

The zymograms with casein as a substrate in the presence or absence of $Ca^{2+}$ (Fig. 4c, d) showed for WE three proteolytic bands of approximately 84, 30, and 27 kDa. In contrast, with E/S products, only a proteolytic band of 30 kDa was detected, while the degradation band of 84 kDa appeared just as a subtle degradation band (Fig. 4d, arrow). The MP inhibitors (EGTA and 1,10-phenanthroline) did not affect the substrate degradation pattern in WE or E/S products, whereas PMSF showed a clear inhibition of all of the degradation bands (Fig. 4c, d, PMSF). TLCK produced a subtle inhibition of the degradation bands of 84 and 30 kDa (Fig. 4c, d). These data suggest that not all SP present in WE are released as E/S products, and the 30-kDa protease detected in both samples was clearly inhibited by PMSF. Interestingly, the bands of 30 and 27 kDa corresponding to SPs were not detected by gelatin zymography (Figs. 1 and 2). Zymograms of WE and E/S products using a mixture of gelatin (0.1%) and casein (0.1%) did not show consistent degradation patterns (data not shown).

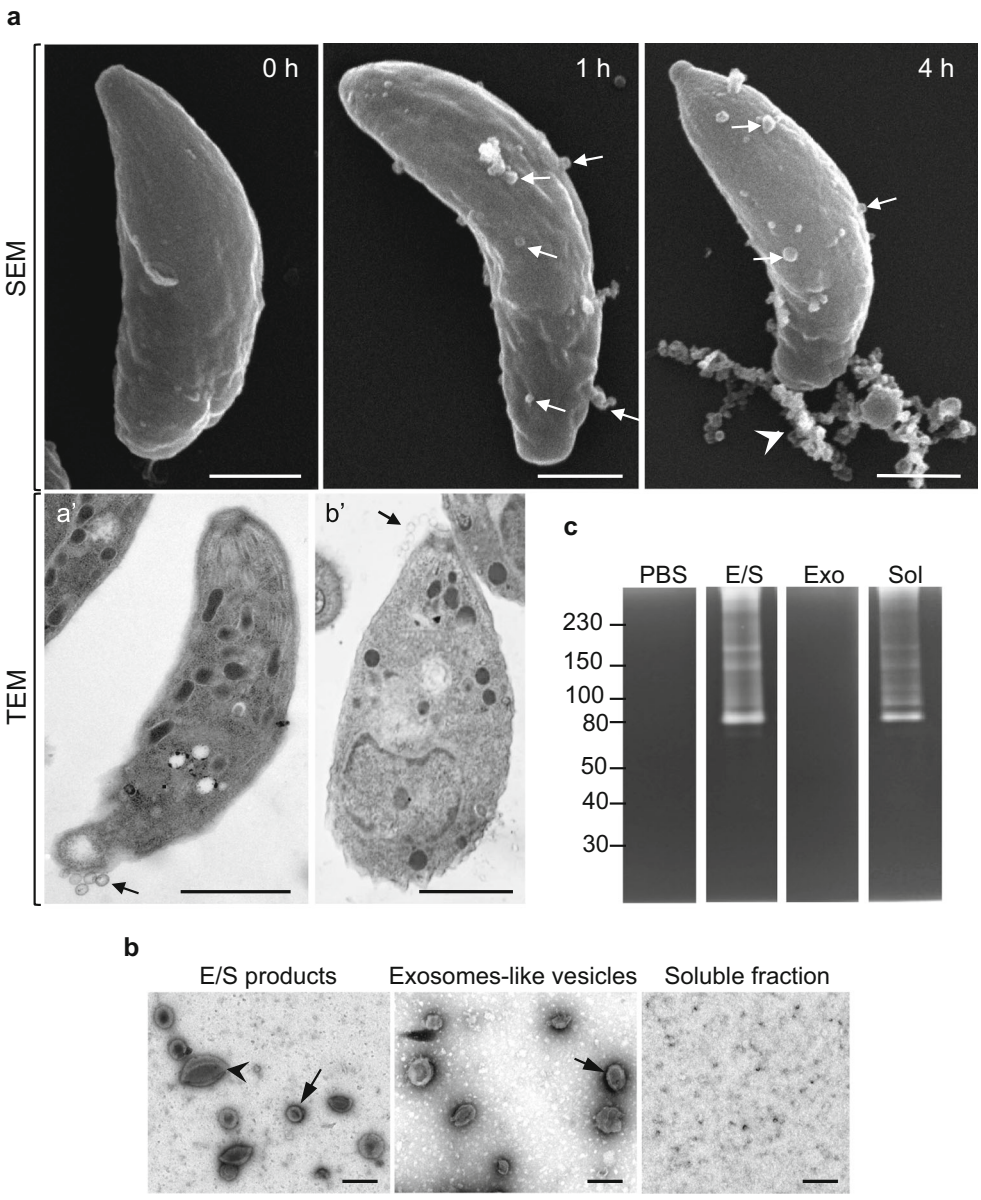


**Fig. 5** E/S products secreted by *Toxoplasma* are constituted by exosome-like vesicles and soluble components enriched with proteases. **a** SEM corresponds to micrographs of tachyzoites maintained in PBS for 0, 1, and 4 h. Scale bars = 1 μm. The arrows indicate the exosome-like vesicles. Arrowhead indicates a exosomes cluster. **a** TEM (a′ and b′) corresponds to micrographs of extracellular tachyzoites maintained in PBS for 4 h before the processing. Scale bar = 1 μm. Arrows indicate the exosome-like vesicles. **b** TEM micrographs by negative staining of E/S products, exosome-like vesicles, and soluble fraction. Arrows indicate the exosome-like vesicles and the arrowhead an ectosome. Scale bar = 200 nm. **c** Gelatin zymography of PBS, in the absence of parasites, E/S products, exosome-like vesicles, and soluble fraction

## Proteases are released as soluble proteins

To analyze the presence of proteases in the exosome-like vesicles, we decided to purify them. First, the ultrastructure of the tachyzoites during the secretion process was analyzed by SEM and TEM. Tachyzoites recently washed and observed by SEM showed a plasma membrane free of vesicles (Fig. 5a, SEM, 0 h). However, parasites maintained under E/S product-harvesting conditions (1 and 4 h) presented numerous exosome-like vesicles associated with the plasma membrane, which increased in number as time passed (Fig. 5a, SEM, arrows). At 4 h, abundant exosome clusters were accumulated at the posterior end of the parasites (Fig. 5a, SEM, arrowhead). In addition, tachyzoites observed by TEM also presented exosome-like vesicles apparently released from the posterior end. Some parasites were observed releasing vesicles directly from the apical end (Fig. 5a, TEM a′ and b′, arrow). None of these parasites showed cytosolic vacuolization nor apoptotic blebbing with nuclei fragmentation, indicating they were viable.

To determine if proteases detected by gelatin zymography are secreted as soluble proteins or associated with exosome-like vesicles, E/S products were fractionated by differential centrifugation to obtain a soluble fraction and an exosomal fraction, which were subsequently analyzed by TEM and by zymography using gelatin as the substrate. Analysis of the total E/S products by TEM showed the presence of exosome-like vesicles in the range of 50–100 nm (Fig. 5b, arrows) and microvesicles morphologically classified as ectosomes of approximately 200 nm, these being less frequent in the sample (Fig. 5b, arrowhead). The fractionation by differential centrifugation of the E/S products produced an exosomal enriched fraction and a soluble fraction that contained only a particulate material, and both were validated by TEM (Fig. 5b). The analysis by gelatin zymography of exosome-like vesicles and soluble fractions showed the proteolytic degradation pattern only with the soluble fraction (Fig. 5c), which indicates that proteases are released by parasites in a soluble manner and are not associated with exosome-like vesicles.

**Table 1** Proteases detected by MS in E/S products of tachyzoites

| Protein | Protein ID | Protease family | Score | MW (kDa) | Sequence coverage | Localization (putative or known) |
|---|---|---|---|---|---|---|
| Cathepsin CPC1 | TGGT1_289620 | Cysteine | 174 | 80 | 8.5 | Secreted[a], DG/PV (Que et al. 2007) |
| Putative ubiquitin specific protease 39 isoform 2 | TGGT1_294360 | Cysteine | 536 | 65 | 37.5 | Nuclear[a,b] |
| Cathepsin CPL | TGGT1_321530 | Cysteine | 402 | 48 | 19.4 | VAC (Miranda et al. 2010), no prediction[a] |
| Putative peptidase M16_ alpha subunit | TGGT1_202680 | Metallo | 198 | 63 | 12.4 | Mitochondria[a,b], secreted[a] |
| Toxolysin TLN4[c] | TGGT1_206510 | Metallo | 1424 | 258 | 31.2 | Micronemes/seceted[a] (Laliberte and Carruthers 2011; Leroux et al. 2015) |
| Peptidase M20D_ amidohydrolase[c] | TGGT1_213520 | Metallo | 224 | 55 | 14.8 | Lysosome[b], mitochondria[a], secreted[a] |
| Peptidase M16 inactive domain-containing protein | TGGT1_214490 | Metallo | 609 | 151 | 18.2 | Cytoplasm[b], nucleus membrane[a], secreted (Leroux et al. 2015) |
| Putative aminopeptidase N | TGGT1_224350A | Metallo | 637 | 136 | 28.2 | Mitochondria[a] |
| Putative aminopeptidase n[c] | TGGT1_224460 | Metallo | 9073 | 109 | 57.3 | No prediction[a] |
| Peptidase family M3 protein[c] | TGGT1_226420 | Metallo | 488 | 76 | 22.0 | ER[b], mitochondria[a], secreted[a] |
| Peptidase M16 inactive domain-containing protein | TGGT1_227948 | Metallo | 1657 | 143 | 42.3 | Mitochondria[a,b], secreted[a] (Leroux et al. 2015) |
| Putative peptidase M16 family protein[c] | TGGT1_236210 | Metallo | 907 | 57 | 31.6 | Mitochondria[b], secreted[a] |
| Peptidase family M3 protein | TGGT1_272670 | Metallo | 147 | 119 | 7.4 | Cytoplasm[b], mitochondria[a] |
| Leucyl aminopeptidase LAP[c] | TGGT1_290,670 | Metallo | 1997 | 84 | 37.3 | Cytoplasm[b] (Jia et al. 2010), secreted (Leroux et al. 2015), mitochondria[a] |
| Aspartyl aminopeptidase | TGGT1_297970 | Metallo | 200 | 57 | 10.2 | Cytoplasm[b] (Zheng et al. 2016), cytoskeleton[a] |
| Rhomboid protease ROM4 | TGGT1_268590 | Serine | 233 | 73 | 2.7 | Membrane[a,b] (Buguliskis et al. 2010) |
| Prolyl endopeptidase | TGGT1_286120 | Serine | 1392 | 93 | 28.5 | Secreted[a] |
| Serine protease | TGGT1_290840 | Serine | 176 | 104 | 10.8 | Membrane[a] |
| Peptidase_T1 family protein | TGGT1_216450 | Threonine | 288 | 28 | 16.5 | Cytoplasm[b], no prediction[a] |

MS and MS/MS spectra were compared using ProteinLynx global SERVER against *Toxoplasma gondii* (GT1 strain, ToxoDB database, Release 38, 19 June 2018). Putative localization of the proteases was predicted by using ProtSecKB database, DeepLoc-1.0 server, or previous reports

*DG* dense granules, *PV* parasitophorous vacuole, *VAC* acidic vacuolar compartment, *ER* endoplasmic reticulum

[a] ProtSecKB database

[b] DeepLoc-1.0 server

[c] Proteases that coincide with degradation bands detected in gelatin zymograms

## Twelve metalloproteases, three serine proteases, and three cysteine proteases were identified in E/S products by MS

MS analysis of the E/S products revealed 19 proteases: 3 CPs, 12 MPs, 3 SPs, and 1 TP (Table 1). The molecular weights of six of the MPs matched the proteolytic bands detected by zymography (Table 1, asterisks**),** and the rest of the MPs were found within a similar range of molecular weights (between 50 and 260 kDa). The protease of 290 kDa and the serine protease detected by gelatin and casein zymography were not identified in the MS analysis. Based on the bioinformatic analysis, several characteristics related to the secretion and intracellular storage of the proteases were determined (Table 1). The detection of proteases previously reported in the E/S products, such as ROM4, TLN4, and CPC1, validated the MS analysis.

## Metalloproteases and serine proteases from E/S products alter the organization of confluent MDCK cells

The effect of the proteases on the host cells was evaluated. The treatment of MDCK cells with E/S products did not induce cell death as demonstrated by SYTOX green dye (Fig. 6a, dead cells arrowed). To determine how the proteases altered the intercellular junctions of confluent MDCK cells, the distribution of the F-actin cytoskeleton was studied after treatment with E/S products. While the control monolayers

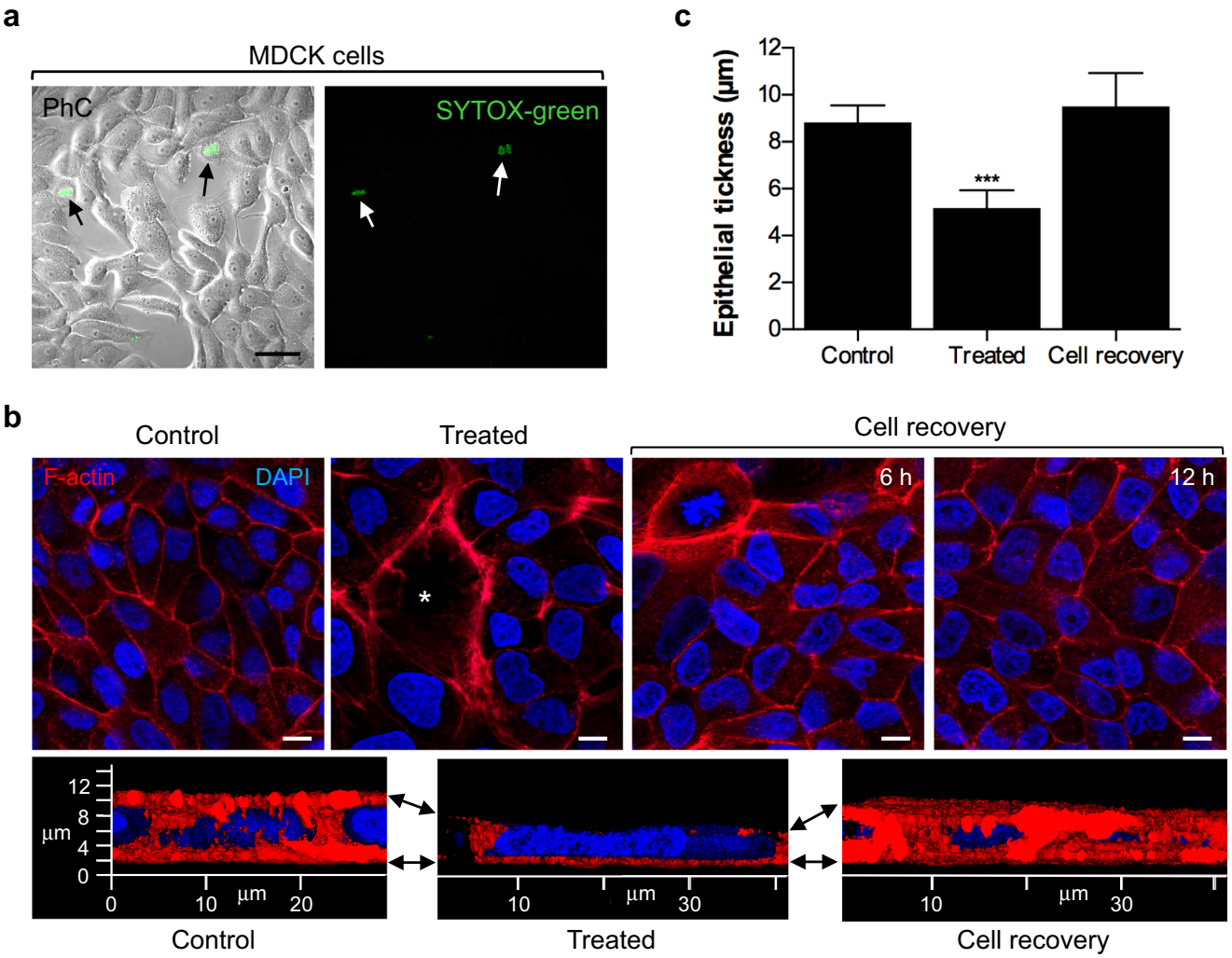


**Fig. 6** Effects of E/S products on viability and distribution of F-actin cytoskeleton in MDCK cells. **a** Staining of MDCK cells with SYTOX green after the treatment with E/S products. Scale bar = 50 µm. **b** Distribution of F-actin (rhodamine phalloidin) in optical sections of MDCK cells: *Control*, cells maintained in 10% FBS-DMEM, *Treated* for 4 h, and *Cell recovery*, after washing the E/S and then maintained for 6 and 12 h in DMEM. Asterisk indicates the aperture in cell-to-cell junctions. Scale bar = 10 µm. Insets at the bottom correspond to transverse optical sections (3D projection) of distribution of F-actin in MDCK cells. Nuclei were stained with DAPI. **c** Mean thickness of control cells, treated cells, and recovered cells. Bars indicate standard deviation. Statistical analysis was performed by using the *T* test with $^{***}p < 0.0005$

(without treatment) presented a normal distribution of F-actin (detected with rhodamine phalloidin) surrounding the cells and along the epithelium (Fig. 6b, Control), in cell monolayers exposed to the E/S products, there was an evident disorganization of the F-actin cytoskeleton, with apertures in cell-to-cell junctions and a thinning of the epithelium (Fig. 6b, Treated, asterisk). 3D projection of Z sections (Fig. 6b, bottom) provided an additional perspective about the epithelial thickness; control cells measured approximately 9 μm (mean), while cells exposed to E/S products had a reduction to approximately 5 μm (mean) **(**Fig. 6b, bottom and c, Treated**)**. When the E/S products were washed out from the cells, all of the alterations reverted to a normal appearance in both epithelial thickness and cell morphology (Fig. 6b, c, Cell recovery).

Incubation of MDCK cells with supernatant harvested from glutaraldehyde-fixed tachyzoites did not alter the monolayer morphology (data not shown).

The effect of the E/S products was evaluated on confluent MDCK monolayers by SEM (Fig. 7). While untreated MDCK cells remained as a continuous monolayer with abundant apical microvilli of similar sizes homogenously distributed (Fig. 7a–c, DMEM), the exposure to E/S products for different times (1, 2, and 4 h) produced a progressive alteration in the intercellular junctions with gaps between neighboring cells and the presence of thin membrane elongations at the basolateral membrane, as well as shortening of the apical microvilli and a diminution in their number (Fig. 7a–c, E/S 1, 2, and 4 h). These effects were partially prevented when E/S products were preincubated with inhibitors for MPs (1,10-phenanthroline) or SPs (PMSF) and then added to the cells (Fig. 7, Phen and PMSF). In the case of PMSF, the cell monolayers showed a maximal similarity with the morphology of untreated cells (Fig. 7, DMEM). EGTA was not tested because its chelating property for $Ca^{2+}$ alters the integrity of intercellular junctions. AP inhibitors were also excluded because their optimal pH is in the acidic range. E-64 was not able to prevent the morphological alterations of MDCK cells induced by E/S products (Fig. 7, E-64). These results suggest that the modifications in the cell-to-cell junctions as well as in microvilli distribution were due to SPs and MPs present in E/S products, although the possibility should not be ruled out that other molecules of the E/S products related or not to the proteases could also induce these cell alterations. Heat denaturation of E/S products inactivated their effect on MDCK cells, suggesting the protein nature of the effector molecules (Fig. 7, Inactivated).

## Discussion

Invasion and tissue dissemination are two of the most important virulence factors of *Toxoplasma*. Tissue dissemination involves the translocation of the parasites through epithelial or endothelial cells, which can occur by means of the following mechanisms: (a) diapedesis of infected leukocytes through the blood vessels (Courret et al. 2006), (b) paracellular transport of extracellular parasites (Barragán et al. 2005), or (c) transcellular transport of extracellular parasites with lysis of the host cell (Mendez and Koshy 2017). In several invasive and systemic pathogens, proteases have been described to play a key role in tissue dissemination (Piña-Vázquez et al. 2012). In previous reports, three *Toxoplasma* MPs were found by gelatin zymography in tachyzoites (RH strain) isolated from infected mice: a 42-kDa MP detected in rhoptries, an 80-kDa MP reported in E/S products but not in WE, and a 72-kDa MP that was not further characterized (Ahn et al. 2001; Song and Nam 2003). The function of such proteases has not been determined yet. In addition, it has been shown that inhibitors for SP and CP block the in vitro invasion by *Toxoplasma*, although the precise mechanism in which they are involved remains unknown (Que et al. 2002).

In the present work, proteases of *Toxoplasma* were characterized in detail. We standardized the optimal conditions to detect the proteases by zymography and identified them based on their sensitivity to inhibitors specific to defined proteases families. In WE from tachyzoites (RH strain), at least nine proteolytic bands sensitive to MP inhibitors were identified (290, 254, 199, 172, 110, 84, 75, 59, and 50 kDa). The same proteolytic pattern was observed in E/S products. When casein was used as a substrate, three SPs of approximately 27, 30, and 84 kDa were detected in WE and two of them were detected in the E/S products (30 and 84 kDa).

Recently, 49 genes codifying for MPs and their respective transcripts were reported in tachyzoites (RH strain), although their protein expression, function, localization, and biochemical properties have not been characterized (Escotte-Binet et al. 2018). Because the number of MPs detected by zymography in both sources (WE and E/S products) does not correspond to the 49 transcripts of the MPs, it is possible that not all of them are expressed at the protein level or they rely on specific induction requirements for their synthesis and secretion. If they were secreted, it remains possible that the amount of synthesized protein would limit their detection by zymography, even at the optimal detection conditions here standardized. Hence, it is possible that the MPs detected here by zymography are the most abundant proteases or the most active. It is also important to consider that each degradation band detected by zymography does not necessarily correspond to a specific protease, particularly in the thick degradation bands (of approximately 84, 254, and 290 kDa). It is possible that these bands contain distinct proteases with similar molecular weights, and therefore, an analysis by 2D zymography would clarify this point. We discarded the possibility that the proteases detected were oligomers since incubation with urea did not modify the zymogram pattern. Additionally, there is the possibility that some degradation bands could appear as a breakdown product of a protease with a high molecular weight. According to the results of the azocasein degradation, we suggest

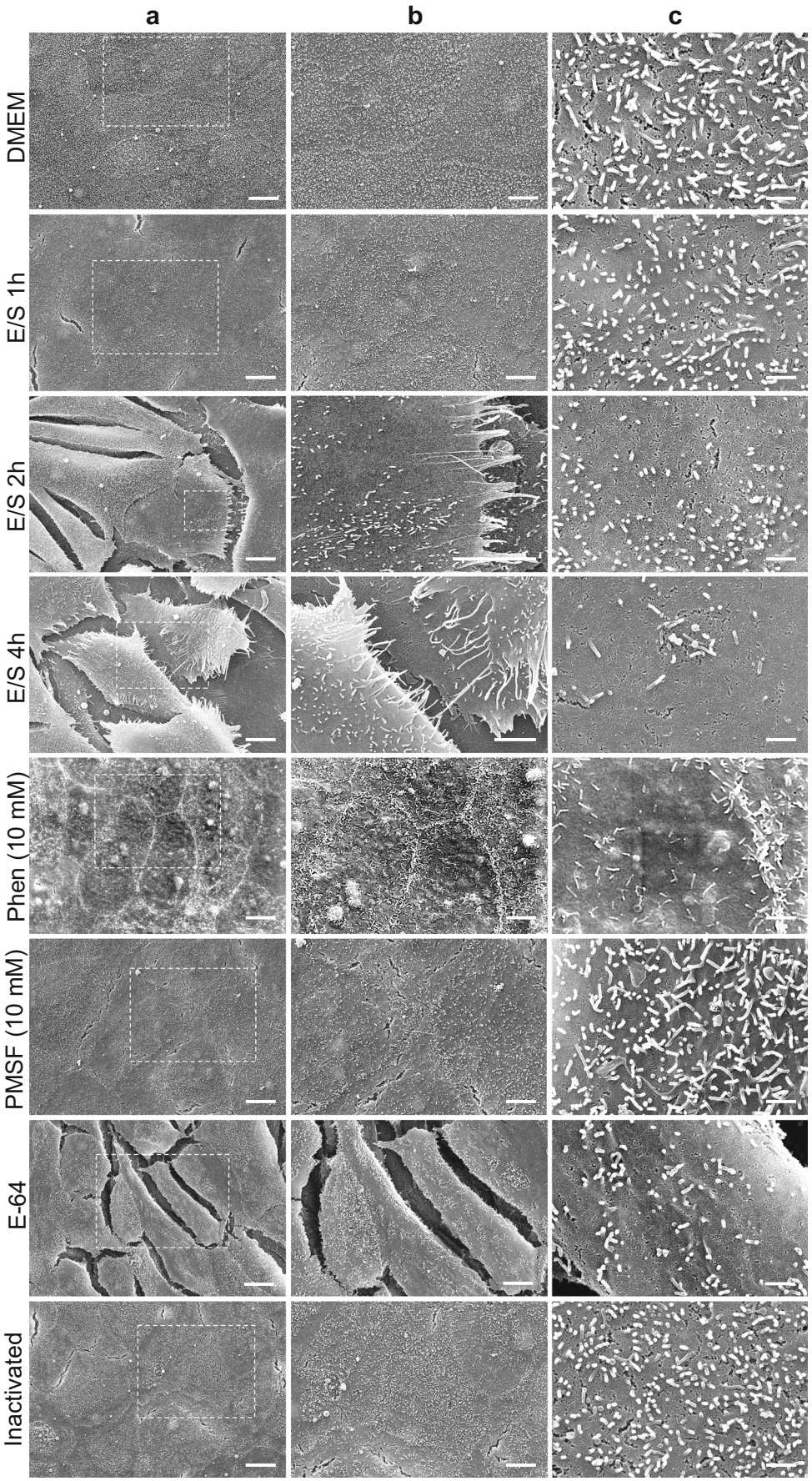
a
b
c
DMEM
E/S 1h
E/S 2h
E/S 4h
Phen (10 mM)
PMSF (10 mM)
E-64
Inactivated

◀ **Fig. 7** E/S products affect the integrity of MDCK monolayers through the action of metalloproteases and serine proteases. SEM micrographs of MDKC monolayers treated with DMEM, for 4 h before processing; E/S products for 1, 2, and 4 h. E/S products were incubated with 1,10-phenanthroline (Phen), PMSF, and E-64 for 1 h, precipitated, and then added to the MDCK confluent cultures. *Inactivated* corresponds to E/S products previously inactivated by heat and then added to the MDCK cells. Frames indicate magnified zones. Set c corresponds to high magnifications of the microvilli. Scale bars in **a** = 10 μm, **b** = 5 μm, and **c** = 1 μm

that some MPs could be dependent on SPs for their activation due to the activity of PMSF overlapping with Phen activity. Therefore, if SPs are inhibited by PMSF as a consequence, the activity of MPs would be diminished.

The characterization of the fractions generated after differential centrifugations of E/S products produced a soluble fraction and a fraction enriched with vesicles with morphological characteristics of exosomes described by a previous report (Cocucci and Meldolesi 2015). The proteolytic analysis demonstrated that all of the proteases detected by zymography were present in the soluble fraction but not in the exosomal fraction. The precise intracellular origin of the proteases and their secretion mechanism remains to be determined.

MS analysis of the E/S products identified 19 proteases, 3 CPs, 12 MPs, 3 SPs, and 1 TP, among which 6 of the MPs coincided with the proteolytic bands detected by zymography. Some of the MPs from tachyzoites (RH strain) described here coincided with the ones described in a recent report (Escotte-Binet et al. 2018). In addition, in the proteome of E/S products from tachyzoites isolated from cell culture (Leroux et al. 2015), only five proteases were detected, including the SP TgSUB1 (TGGT1_204050, 85 kDa), and four MPs: TLN4 (TGGT1_206510, 257 kDa), leucyl aminopeptidase LAP (TGGT1_290670, 83 kDa), and two peptidases from the M16 inactive domain-containing protein (TGGT1_227948, 143 kDa and TGGT1_214490, 149 kDa) (Leroux et al. 2015). TgCPL, a CP related to the protein maturing process, was also detected in the E/S products, although it has been reported to be stored within a VAC compartment (Dou et al. 2013). The MP of 110 kDa detected here seems to correspond to a protein previously reported (Berthonneau et al. 2000) and described in the transcriptomic profile (TGME49_224460) (Escotte-Binet et al. 2018), although its function remains to be determined. In addition, the MP of 84 kDa, observed with maximal activity by zymography, was identified by MS analysis as the leucyl aminopeptidase LAP (TGME49 290,670), which was originally reported and partially characterized as a cytosolic metal cation divalent protease (Jia et al. 2010) but recently described as part of the E/S products (Leroux et al. 2015). The aspartyl aminopeptidase (TgAAP) (TgGT_1297970) has been functionally analyzed. Its knockout inhibited the invasion and replication of the parasite (Zheng et al. 2016). The function or characterization of the other proteases found here in the E/S products has not been studied. Importantly, proteases well known to be secreted/released such as TLN4, ROM4, and CPC1 were detected in our analysis, validating the MS analysis of the E/S products.

Although gel zymography is an excellent approach for the functional characterization of proteolytic enzymes and is a tool broadly used in several cell models, the absence of CPs in the E/S products from *T. gondii* proteases may be due to the following possibilities: (a) the CPs in the sample were degraded during the sample processing, (b) the conditions tested for the activation and detection of CPs are not the optimal to activate the CPs, and/or (c) the zymography assay used in this study is not sensitive enough for the detection of all classes of proteases. Thus, alternative approaches must be considered in order to extend the characterization of the CPs identified by MS in the E/S products.

MDCK cell monolayer has been widely used to study parasite dissemination in vitro, as it preserves most of the molecular and biological properties of a typical epithelium (Rothen-Rutishauser et al. 1998). It was previously reported that tachyzoites (RH strain) maintained in human foreskin fibroblasts are able to transmigrate through MDCK cells in vitro via a paracellular pathway without altering the integrity of the cell monolayer (Barragán et al. 2005). In our study, the exposure of the MDCK cells to E/S products harvested from tachyzoites (RH strain) obtained from infected mice produced clear modifications in the confluence of the MDCK cells with separation of the cells and a reduction in the length and number of the apical microvilli. These alterations can be attributed to the effect of MPs and SPs present in E/S products because the specific inhibitors 1,10-phenanthroline (for MPs) and PMSF (for SPs) prevented the mentioned effect. Furthermore, the alterations of the cell monolayer were reversed as the E/S products were removed and the cells were thoroughly washed and maintained in culture medium. The denaturing of the E/S products by heat or by chemical fixation and the consequent blockade of the effect on the cell monolayer indicated that the molecules involved are proteins. Although the separation of the epithelium was prevented with treatment with Phen, the microvilli showed certain modifications, perhaps due to the effect of MPs or other proteases that were not inhibited. To our knowledge, this is the first time that the proteolytic activity from *Toxoplasma* E/S products has been related to morphological disruption of an epithelial cell monolayer, an in vitro model of invasion. Nonetheless, the possibility that the proteases might activate other effector molecules contributing to the observed alterations cannot be ruled out. The role of proteases in tissue dissemination needs to be confirmed by analysis of their effect in epithelial transmigration techniques and by transepithelial resistance assays. One approach to determine the participation of proteases in tissue dissemination is the use of *knockdown* parasites for defined proteases, although the use of proteases purified by affinity chromatography and the use of recombinant proteases with

preserved proteolytic activities are also very valuable and interesting approach.

Because the E/S products were harvested from resting parasites maintained in PBS, it is possible that the proteases are secreted through a constitutive secretion process. However, it is also possible that as the parasites were harvested from infected mice, they would already be primed for the secretion of virulence factors. To test this possibility, proteases from E/S products must be studied in parasites maintained under culture conditions in which biological inducers are absent or minimally expressed. The presence of the various proteases in the E/S products suggests that these would facilitate the invasion and/or the tissue dissemination of *Toxoplasma*. The role of MPs in degradation of the ECM has been reported in several intracellular and extracellular pathogens as a strategy for tissue dissemination (Piña-Vázquez et al. 2012; Potempa and Potempa 2012). Moreover, it has been reported that *Toxoplasma* (Buache et al. 2007) induces the release of MMPs from the host cell in order to facilitate their tissue spreading by degradation of the ECM.

The cellular and biochemical analysis of proteases in *Toxoplasma* and the study of their effects on cells and tissues, as well as their participation in tissue dissemination, lead us to consider them as potential virulence factors. In many parasites, proteases play a crucial role in diverse processes such as invasion, host protein degradation, and evasion of host immune responses, among others, which make proteases an excellent target for vaccine design (Siqueira-Neto et al. 2018). To date, the proteases in *Toxoplasma* have been demonstrated to have an immune-protector role (Han et al. 2017; Zhao et al. 2017). Herein, our results open the possibility of studying *Toxoplasma* proteases in the context of immuno-protection or immuno-diagnosis. Protease characterization in other genotypic strains such as type II and type III would provide valuable information to understand their virulence differences, the formation of tissue cysts, and their differential organ infection.

**Acknowledgements** This research was supported by grants from Fundación Miguel Alemán A.C. and by Centro de Investigación y de Estudios Avanzados del Instituto Politécnico Nacional (CINVESTAV-IPN) to RMF and scholarships from Consejo Nacional de Ciencia y Tecnología (CONACyT, México) to CJRF and RCM (296155 and 295997, respectively). We thank R. Mondragón-González from Departamento de Genética y Biología Molecular (CINVESTAV-IPN) for his comments and A. Chagolla-López from the Departamento de Biotecnología y Bioquímica (CINVESTAV-IPN, Irapuato) for her technical support.

## Compliance with ethical standards

**Conflict of interest** The authors declare that they have no conflicts of interest with the contents of this article.



## References

Ahn HJ, Song KJ, Son ES, Shin JC, Nam HW (2001) Protease activity and host cell binding of the 42-kDa rhoptry protein from *Toxoplasma gondii* after secretion. Biochem Biophys Res Commun 287:630–635

Almagro Armenteros JJ, Sonderby CK, Sonderby SK, Nielsen H, Winther O (2017) DeepLoc: prediction of protein subcellular localization using deep learning. Bioinformatics 33:3387–3395

Barragán A, Sibley LD (2002) Transepithelial migration of *Toxoplasma gondii* is linked to parasite motility and virulence. J Exp Med 195:1625–1633

Barragán A, Sibley LD (2003) Migration of *Toxoplasma gondii* across biological barriers. Trends Microbiol 11:426–430

Barragán A, Brossier F, Sibley LD (2005) Transepithelial migration of *Toxoplasma gondii* involves an interaction of intercellular adhesion molecule 1 (ICAM-1) with the parasite adhesin MIC2. Cell Microbiol 7:561–568

Berthonneau J, Rodier MH, El Moudni B, Jacquemin JL (2000) *Toxoplasma gondii*: purification and characterization of an immunogenic metallopeptidase. Exp Parasitol 95:158–162

Buache E, Garnotel R, Aubert D, Gillery P, Villena I (2007) Reduced secretion and expression of gelatinase profile in *Toxoplasma gondii*-infected human monocytic cells. Biochem Biophys Res Commun 359:298–303

Buguliskis JS, Brossier F, Shuman J, Sibley LD (2010) Rhomboid 4 (ROM4) affects the processing of surface adhesins and facilitates host cell invasion by *Toxoplasma gondii*. PLoS Pathog 6:e1000858

Chaparro JD, Cheng T, Tran UP, Andrade RM, Brenner SBT, Hwang G, Cohn S, Hirata K, McKerrow JH, Reed SL (2018) Two key cathepsins, TgCPB and TgCPL, are targeted by the vinyl sulfone inhibitor K11777 in in vitro and in vivo models of toxoplasmosis. PLoS One 13:e0193982

Cocucci E, Meldolesi J (2015) Ectosomes and exosomes: shedding the confusion between extracellular vesicles. Trends Cell Biol 25:364–372

Coelho DF, Saturnino TP, Fernandes FF, Mazzola PG, Silveira E, Tambourgi EB (2016) Azocasein substrate for determination of proteolytic activity: reexamining a traditional method using bromelain samples. Biomed Res Int 2016:8409183

Coffey MJ, Sleebs BE, Uboldi AD, Garnham A, Franco M, Marino ND, Panas MW, Ferguson DJ, Enciso M, O'Neill MT, Lopaticki S, Stewart RJ, Dewson G, Smyth GK, Smith BJ, Masters SL, Boothroyd JC, Boddey JA, Tonkin CJ (2015) An aspartyl protease defines a novel pathway for export of *Toxoplasma* proteins into the host cell. Elife 4:e10809

Conseil V, Soete M, Dubremetz JF (1999) Serine protease inhibitors block invasion of host cells by *Toxoplasma gondii*. Antimicrob Agents Chemother 43:1358–1361

Courret N, Darche S, Sonigo P, Milon G, Buzoni-Gatel D, Tardieux I (2006) CD11c- and CD11b-expressing mouse leukocytes transport single *Toxoplasma gondii* tachyzoites to the brain. Blood 107:309–316

Cuellar P, Hernandez-Nava E, Garcia-Rivera G, Chavez-Munguia B, Schnoor M, Betanzos A, Orozco E (2017) *Entamoeba histolytica* EhCP112 dislocates and degrades Claudin-1 and Claudin-2 at tight junctions of the intestinal epithelium. Front Cell Infect Microbiol 7:372

de Sousa KP, Atouguia J, Silva MS (2010) Partial biochemical characterization of a metalloproteinase from the bloodstream forms of *Trypanosoma brucei brucei* parasites. Protein J 29:283–289

Dou Z, Coppens I, Carruthers VB (2013) Non-canonical maturation of two papain-family proteases in *Toxoplasma gondii*. J Biol Chem 288:3523–3534

Dou Z, McGovern OL, Di Cristina M, Carruthers VB (2014) *Toxoplasma gondii* ingests and digests host cytosolic proteins. MBio 5:e01188–e01114

Escotte-Binet S, Huguenin A, Aubert D, Martin AP, Kaltenbach M, Florent I, Villena I (2018) Metallopeptidases of *Toxoplasma gondii*: in silico identification and gene expression. Parasite 25:26

Gimenez MI, Studdert CA, Sanchez JJ, De Castro RE (2000) Extracellular protease of *Natrialba magadii*: purification and biochemical characterization. Extremophiles 4:181–188

Hajagos BE, Turetzky JM, Peng ED, Cheng SJ, Ryan CM, Souda P, Whitelegge JP, Lebrun M, Dubremetz JF, Bradley PJ (2012) Molecular dissection of novel trafficking and processing of the *Toxoplasma gondii* rhoptry metalloprotease toxolysin-1. Traffic 13:292–304

Han Y, Zhou A, Lu G, Zhao G, Sha W, Wang L, Guo J, Zhou J, Zhou H, Cong H, He S (2017) DNA vaccines encoding *Toxoplasma gondii* Cathepsin C 1 induce protection against toxoplasmosis in mice. Korean J Parasitol 55:505–512

Harker KS, Ueno N, Lodoen MB (2015) *Toxoplasma gondii* dissemination: a parasite's journey through the infected host. Parasite Immunol 37:141–149

Hernández-Gutiérrez R, Ávila-González L, Ortega-López J, Cruz-Talonia F, Gómez-Gutiérrez G, Arroyo R (2004) *Trichomonas vaginalis*: characterization of a 39-kDa cysteine proteinase found in patient vaginal secretions. Exp Parasitol 107:125–135

Heussen C, Dowdle EB (1980) Electrophoretic analysis of plasminogen activators in polyacrylamide gels containing sodium dodecyl sulfate and copolymerized substrates. Anal Biochem 102:196–202

Jia H, Nishikawa Y, Luo Y, Yamagishi J, Sugimoto C, Xuan X (2010) Characterization of a leucine aminopeptidase from *Toxoplasma gondii*. Mol Biochem Parasitol 170:1–6

Khan NA, Siddiqui R (2009) Acanthamoeba affects the integrity of human brain microvascular endothelial cells and degrades the tight junction proteins. Int J Parasitol 39:1611–1616

Lagal V, Binder EM, Huynh MH, Kafsack BF, Harris PK, Diez R, Chen D, Cole RN, Carruthers VB, Kim K (2010) *Toxoplasma gondii* protease TgSUB1 is required for cell surface processing of micronemal adhesive complexes and efficient adhesion of tachyzoites. Cell Microbiol 12:1792–1808

Laliberte J, Carruthers VB (2011) *Toxoplasma gondii* toxolysin 4 is an extensively processed putative metalloproteinase secreted from micronemes. Mol Biochem Parasitol 177:49–56

Leroux LP, Dasanayake D, Rommereim LM, Fox BA, Bzik DJ, Jardim A, Dzierszinski FS (2015) Secreted *Toxoplasma gondii* molecules interfere with expression of MHC-II in interferon gamma-activated macrophages. Int J Parasitol 45:319–332

Li GZ, Vissers JP, Silva JC, Golick D, Gorenstein MV, Geromanos SJ (2009) Database searching and accounting of multiplexed precursor and product ion spectra from the data independent analysis of simple and complex peptide mixtures. Proteomics 9:1696–1719

Li P, Kaslan M, Lee SH, Yao J, Gao Z (2017) Progress in exosome isolation techniques. Theranostics 7:789–804

Louie K, Nordhausen R, Robinson TW, Barr BC, Conrad PA (2002) Characterization of *Neospora caninum* protease, NcSUB1 (NC-P65), with rabbit anti-N54. J Parasitol 88:1113–1119

Madanan MG, Mechoor A (2017) Detection and characterization of bacterial proteinases using zymography. Methods Mol Biol 1626:103–114

McGwire BS, Chang KP, Engman DM (2003) Migration through the extracellular matrix by the parasitic protozoan *Leishmania* is enhanced by surface metalloprotease gp63. Infect Immun 71:1008–1010

Mendez OA, Koshy AA (2017) *Toxoplasma gondii*: entry, association, and physiological influence on the central nervous system. PLoS Pathog 13:e1006351

Miller SA, Thathy V, Ajioka JW, Blackman MJ, Kim K (2003) TgSUB2 is a *Toxoplasma gondii* rhoptry organelle processing proteinase. Mol Microbiol 49:883–894

Miranda K, Pace DA, Cintron R, Rodrigues JC, Fang J, Smith A, Rohloff P, Coelho E, de Haas F, de Souza W, Coppens I, Sibley LD, Moreno SN (2010) Characterization of a novel organelle in *Toxoplasma gondii* with similar composition and function to the plant vacuole. Mol Microbiol 76:1358–1375

Mondragón R, Frixione E (1996) Ca(2+)-dependence of conoid extrusion in *Toxoplasma gondii* tachyzoites. J Eukaryot Microbiol 43:120–127

Monte JFS, Moreno CJG, Monteiro J, de Oliveira Rocha HA, Ribeiro AR, Silva MS (2017) Use of zymography in trypanosomiasis studies. Methods Mol Biol 1626:213–220

Neuhoff V, Arold N, Taube D, Ehrhardt W (1988) Improved staining of proteins in polyacrylamide gels including isoelectric focusing gels with clear background at nanogram sensitivity using Coomassie Brilliant Blue G-250 and R-250. Electrophoresis 9:255–262

Nogueira de Melo AC, de Souza EP, Elias CG, dos Santos AL, Branquinha MH, d'Avila-Levy CM, dos Reis FC, Costa TF, Lima AP, de Souza Pereira MC, Meirelles MN, Vermelho AB (2010) Detection of matrix metallopeptidase-9-like proteins in *Trypanosoma cruzi*. Exp Parasitol 125:256–263

Nogueira AR, Leve F, Morgado-Diaz J, Tedesco RC, Pereira MC (2016) Effect of *Toxoplasma gondii* infection on the junctional complex of retinal pigment epithelial cells. Parasitology 143:568–575

Oliveira-Jr FO, Alves CR, Silva FS, Cortes LM, Toma L, Boucas RI, Aguilar T, Nader HB, Pereira MC (2013) *Trypanosoma cruzi* heparin-binding proteins present a flagellar membrane localization and serine proteinase activity. Parasitology 140:171–180

Piña-Vázquez C, Reyes-López M, Ortíz-Estrada G, de la Garza M, Serrano-Luna J (2012) Host-parasite interaction: parasite-derived and -induced proteases that degrade human extracellular matrix. J Parasitol Res 2012:1–24

Potempa M, Potempa J (2012) Protease-dependent mechanisms of complement evasion by bacterial pathogens. Biol Chem 393: 873–888

Prato M, Giribaldi G, Polimeni M, Gallo V, Arese P (2005) Phagocytosis of hemozoin enhances matrix metalloproteinase-9 activity and TNF-alpha production in human monocytes: role of matrix metalloproteinases in the pathogenesis of falciparum malaria. J Immunol 175: 6436–6442

Que X, Ngo H, Lawton J, Gray M, Liu Q, Engel J, Brinen L, Ghosh P, Joiner KA, Reed SL (2002) The cathepsin B of *Toxoplasma gondii*, toxopain-1, is critical for parasite invasion and rhoptry protein processing. J Biol Chem 277:25791–25797

Que X, Engel JC, Ferguson D, Wunderlich A, Tomavo S, Reed SL (2007) Cathepsin Cs are key for the intracellular survival of the protozoan parasite, *Toxoplasma gondii*. J Biol Chem 282:4994–5003

Rothen-Rutishauser B, Kramer SD, Braun A, Gunthert M, Wunderli-Allenspach H (1998) MDCK cell cultures as an epithelial in vitro model: cytoskeleton and tight junctions as indicators for the definition of age-related stages by confocal microscopy. Pharm Res 15: 964–971

Saboia-Vahia L, Borges-Veloso A, Mesquita-Rodrigues C, Cuervo P, Dias-Lopes G, Britto C, Silva AP, De Jesus JB (2013) Trypsin-like serine peptidase profiles in the egg, larval, and pupal stages of *Aedes albopictus*. Parasit Vectors 6:50

Saboia-Vahia L, Cuervo P, Borges-Veloso A, de Souza NP, Britto C, Dias-Lopes G, De Jesus JB (2014) The midgut of *Aedes albopictus* females expresses active trypsin-like serine peptidases. Parasit Vectors 7:253

Sampieri CL, de la Pena S, Ochoa-Lara M, Zenteno-Cuevas R, Leon-Cordoba K (2010) Expression of matrix metalloproteinases 2 and 9 in human gastric cancer and superficial gastritis. World J Gastroenterol 16:1500–1505

Schuindt SH, Oliveira BC, Pimentel PM, Resende TL, Retamal CA, DaMatta RA, Seipel D, Arnholdt AC (2012) Secretion of multiprotein migratory complex induced by *Toxoplasma gondii* infection in macrophages involves the uPA/uPAR activation system. Vet Parasitol 186:207–215

Shevchenko A, Tomas H, Havlis J, Olsen JV, Mann M (2006) In-gel digestion for mass spectrometric characterization of proteins and proteomes. Nat Protoc 1:2856–2860

Siqueira-Neto JL, Debnath A, McCall LI, Bernatchez JA, Ndao M, Reed SL, Rosenthal PJ (2018) Cysteine proteases in protozoan parasites. PLoS Negl Trop Dis 12:e0006512

Song KJ, Nam HW (2003) Protease activity of 80 kDa protein secreted from the apicomplexan parasite *Toxoplasma gondii*. Korean J Parasitol 41:165–169

Tenter AM, Heckeroth AR, Weiss LM (2000) *Toxoplasma gondii*: from animals to humans. Int J Parasitol 30:1217–1258

Tork SE, Shahein YE, El-Hakim AE, Abdel-Aty AM, Aly MM (2016) Purification and partial characterization of serine-metallokeratinase from a newly isolated Bacillus pumilus NRC21. Int J Biol Macromol 86:189–196

Wilkesman J (2017) Cysteine protease zymography: brief review. Methods Mol Biol 1626:25–31

Zhao G, Zhou A, Lv G, Meng M, Sun M, Bai Y, Han Y, Wang L, Zhou H, Cong H, Zhao Q, Zhu XQ, He S (2013) *Toxoplasma gondii* cathepsin proteases are undeveloped prominent vaccine antigens against toxoplasmosis. BMC Infect Dis 13:207

Zhao G, Song X, Kong X, Zhang N, Qu S, Zhu W, Yang Y, Wang Q (2017) Immunization with *Toxoplasma gondii* aspartic protease 3 increases survival time of infected mice. Acta Trop 171:17–23

Zheng J, Cheng Z, Jia H, Zheng Y (2016) Characterization of aspartyl aminopeptidase from *Toxoplasma gondii*. Sci Rep 6:34448